Soft Matter

Suppression of hypersynchronous network activity in cultured cortical neurons using an ultrasoft silicone scaffold

Journal:	*Soft Matter*
Manuscript ID	SM-ART-12-2019-002432.R1
Article Type:	Paper
Date Submitted by the Author:	05-Feb-2020
Complete List of Authors:	Sumi, Takuma; Tohoku University, Research Institute of Electrical Communication Yamamoto, Hideaki; Tohoku University, WPI-Advanced Institute for Materials Research; Tohoku University, Research Institute of Electrical Communication Hirano-Iwata, Ayumi; Tohoku University, WPI-Advanced Institute for Materials Research; Tohoku University, Research Institute of Electrical Communication

SCHOLARONE™
Manuscripts

1 **Suppression of hypersynchronous network activity in**

2 **cultured cortical neurons using an ultrasoft silicone scaffold**

3

4 Takuma Sumi[a], Hideaki Yamamoto*[ab], and Ayumi Hirano-Iwata[ab]

5

6 *[a]Research Institute of Electrical Communication, Tohoku University, 2-1-1 Katahira, Aoba-ku,*

7 *Sendai 980-8577, Japan. E-mail: hideaki.yamamoto.e3@tohoku.ac.jp*

8 *[b]WPI-Advanced Institute for Materials Research (WPI-AIMR), Tohoku University, 2-1-1*

9 *Katahira, Aoba-ku, Sendai 980-8577, Japan*

Abstract

The spontaneous activity pattern of cortical neurons in dissociated culture is characterized by burst firing that is highly synchronized among a wide population of cells. The degree of synchrony, however, is excessively higher than that in cortical tissues. Here, we employed polydimethylsiloxane (PDMS) elastomers to establish a novel system for culturing neurons on a scaffold with an elastic modulus resembling brain tissue, and investigated the effect of the scaffold's elasticity on network activity patterns in cultured rat cortical neurons. Using whole-cell patch clamp to assess the scaffold effect on the development of synaptic connections, we found that the amplitude of excitatory postsynaptic current, as well as the frequency of spontaneous transmissions, was reduced in neuronal networks grown on an ultrasoft PDMS with an elastic modulus of 0.5 kPa. Furthermore, the ultrasoft scaffold was found to suppress neural correlations in the spontaneous activity of the cultured neuronal network. The dose of GsMTx-4, an antagonist of stretch-activated cation channels (SACs), required to reduce the generation of the events below 1.0 event/min on PDMS substrates was lower than that for neurons on a glass substrate. This suggests that the difference in the baseline level of SAC activation is a molecular mechanism underlying the alteration in neuronal network activity depending on scaffold stiffness. Our results demonstrate the potential application of PDMS with biomimetic elasticity as cell-culture scaffold for bridging the *in vivo-in vitro* gap in neuronal systems.

29   **Main text**

30   **1. Introduction**

31   *In vitro* modelling of *in vivo* multicellular functions is essential in biology and medicine not

32   only for basic studies but also for applied research, such as the screening of candidate molecules

33   in drug development.[1,2] In fields such as cardiology and oncology, cultured-cell models have

34   been established and are used in disease modelling and toxicity assays.[1,3] However, in

35   neuroscience, cortical and hippocampal neurons in dissociated culture generate a

36   non-physiological activity characterized by globally synchronized burst firing, often referred to

37   as 'network bursts'.[4-7] This activity pattern is significantly different from that observed in an

38   animals' cortex or hippocampus, which is highly complex both spatially and temporally.[8,9] Such

39   complexity in neural activity is important, as it underlies the computational capacity of the

40   neuronal networks.[10,11]

41   Several approaches have been taken to suppress the globally synchronized bursting in

42   cultured neuronal networks. For instance, it has been shown that the synchronized bursts are

43   inhibited and the complexity in the spontaneous activity is upregulated by growing cultured

44   neurons on micropatterned surfaces to induce a network architecture such as those observed in

45   the *in vivo* networks.[12] The role of external inputs in shaping the spontaneous dynamics of the

46   cultured neural networks has also been investigated both experimentally and computationally,

47   showing that chronic application of external stimulus that resembles thalamic input decorrelates

48   cortical neuronal network activity.[13-15] Furthermore, pharmacological blockade of an

49   AMPA-type glutamate receptor with CNQX at a dose below its IC_{50} reduces the spatial extent

50   of the burst spreading,[5] possibly through a reduction in the excitatory synaptic strength that is

51   excessively strong in cultured neurons as compared to the *in vivo* cortex.[16-18]

52   Another major difference between the *in vitro* and *in vivo* neuronal networks is the

53   mechanical property of their scaffolds. Cultured neurons are usually grown on a polystyrene or

54   glass substrate, whose elastic moduli, E, are in the order of GPa.[19,20] In contrast, the brain is the

55   softest tissue in an animals' body, with an E below 1 kPa.[21] Several studies on non-neuronal

56   cells have pointed to the importance of culturing cells on a scaffold with biomimetic elasticity.

57   For instance, mesenchymal stem cells commit to the lineage specified by scaffold elasticity.[22]

58   Furthermore, the expression of chondrocyte phenotype is stabilized when cultured on a scaffold

59   with an E of 5.4 kPa, similar to that of the *in vivo* environment.[23] Based on these observations,

60   we hypothesized that the non-physiological synchronized bursting in cultured neuronal

61   networks could be suppressed by growing neurons on a biomimetic scaffold.

62   In this work, we established a biomimetic culture platform using polydimethylsiloxane

63   (PDMS) that is as soft as brain tissue (i.e. $E \sim 0.5$ kPa). PDMS is a well-established

64   biocompatible material, whose elasticity can be tuned in a wide range, from ~0.1 kPa to tens of

65   MPa by choosing the precursors and changing their mixing ratio.[24,25] It also offers several

66   advantages over more commonly used materials (e.g. polyacrylamide), such as being

67   compatible with surface modification techniques, being electrically insulating, and having a

68   long shelf life.[26] Primary rat cortical neurons, one of the most well-established systems in

69   dissociated culture of neuronal cells, were cultured on the PDMS substrate, and the effect of the

70   scaffold's stiffness on synaptic strength and the complexity of the neuronal network activity was

71   assessed using whole-cell patch-clamp recording and fluorescent calcium imaging, respectively.

72   We show that the excitatory synapses are weakened on the softer substrates and that the

73   neuronal correlation in spontaneous network activity is significantly reduced on the PDMS

74   substrate with an $E \sim 0.5$ kPa. The underlying molecular mechanism responsible for the

75   stiffness-dependent modulation on spontaneous network activity is pharmacologically explored

76   by blocking stretch-activated cation channels (SACs).

77

78

79   **2. Experimental**

80   **2.1 Mechanical characterization of the PDMS**

81   PDMS was prepared using Sylgard 184 (Dow Corning; mixing ratio = 50:1) and Sylgard 527

82   (Dow Corning; mixing ratio = 5:4). For each PDMS, 200 g of the mixtures were poured in a

83   glass petri dish (diameter, 90 mm; height, 60 mm), degassed in a vacuum chamber, and cured in

84   an oven (AS-ONE SONW-450S) for two days at 80 °C.

85   The elastic modulus of the PDMS was determined by the spherical indentation method

86   (Fig. 1a) following Zhang *et al.*[27,28] Briefly, a chromium steel ball of 3.175-mm radius (R) was

87   attached onto the load cell of the Instron 5943 Universal Testing System. The depth

88   (δ)-indentation load (P) curves were measured (Fig. 1b), and the elastic moduli, E, were

89   determined by fitting the load curves to the following equation:

$$P = \frac{16}{9}E\sqrt{R\delta}\delta\left(1 - 0.15\frac{\delta}{R}\right). \tag{1}$$

90

91   **2.2 PDMS substrates for neuronal culture**

92   Glass coverslips (Matsunami C018001; diameter, 18 mm; thickness 0.17 mm) were first cleaned

93   by sonication in 99.5% ethanol and rinsed two times in Milli-Q grade water. After a thorough

94   mixing of the two PDMS components and subsequent degassing, 100 μL of the mixture was

95   drop casted on the coverslip. PDMS was then cured in an oven for 11 h at 80 °C.

96

97   **2.3 Contact angle measurement**

98   The hydrophilicity of the surfaces was characterized by measuring the water contact angle.

99   Using the LSE-B100 equipment (NiCK Corporation, Japan), a 0.5-μL water droplet was

100   dropped onto the substrate and was imaged from the side. The contact angle of the droplet was

101   measured using the i2win software (NiCK Corporation, Japan). Three samples were prepared

102   for each condition, and measurements were performed at three different positions for each

103   sample.

104

105   **2.4 Cell culture**

106   For cell culturing, the PDMS substrate was first treated in air plasma (Yamato PM-100) for 10 s

107   and was sterilized under UV light (Toshiba GL-15; wavelength, ~253.7 nm) for 60 min. The

108   exposure to UV light itself did not affect the surface properties, as confirmed by water contact

109   angle measurements (data not shown). In order to promote the adhesion of neuronal cells, the

110   surface of the PDMS was then coated with poly-D-lysine (PDL; Sigma P-0899) by floating the

111   sample upside-down on a phosphate-buffered saline (Gibco 14190-144) containing 50 μg/mL

112   PDL overnight. The sample was then rinsed two times in sterilized water and dried in air inside

113   a laminar flow hood. One day prior to cell plating, the sample was immersed in the plating

114   medium [minimum essential medium (Gibco 11095-080) + 5% foetal bovine serum + 0.6%

115   D-glucose] and stored in a CO_2 incubator (37 ºC). Glass coverslips without the PDMS layer

116   were used in control experiments. These were prepared by cleaning coverslips in ethanol and

117   water, treating the surface with air plasma (60 s), UV-sterilization (60 min), and subsequent

118   coating with PDL (overnight).

119   Rat cortical neurons from 18-d old embryos were used in our experiments. All

120   procedures comply with the Regulations for Animal Experiments and Related Activities at

121   Tohoku University and were approved by the Center for Laboratory Animal Research, Tohoku

122   University (approval number: 2017AmA-001-1). After dissection of the cortical tissues and cell

123   dispersion, the cells were plated on the samples immersed in the plating medium. After a 3 h

124   incubation, the medium was changed to Neurobasal medium [Neurobasal (Gibco 21103-049) +

125   2% B-27 supplement (Gibco 17504-044) + 1% GlutaMAX-I (Gibco 3505-061)]. Half of the

126   medium was replaced with fresh Neurobasal medium at 4 and 8 days of the culture.

127

128   **2.5 Electrophysiology**

129   Whole-cell patch-clamp recordings (HEKA EPC-10) were performed on neurons at 14−18 DIV

130   under the voltage-clamp mode (holding potential, -70 mV). Signals were sampled at 20 kHz and

131   filtered with 10 kHz and 2.9 kHz Bessel filters. Recordings were performed at room

132   temperature. The intracellular solution contained: 146.3 mM KCl, 0.6 mM $MgCl_2$, 4 mM

133   ATP-Mg, 0.3 mM GTP-Na, 5 U/mL creatine phosphokinase, 12 mM phosphocreatine, 1 mM

134   EGTA, and 17.8 mM HEPES (pH 7.4). The extracellular solution for the recording contained:

135   140 mM NaCl, 2.4 mM KCl, 10 mM HEPES, 10 mM glucose, 2 mM $CaCl_2$, and 1 mM $MgCl_2$

136   (pH 7.4).[18] The $GABA_A$ receptor antagonist, bicuculline (Sigma 14343; 10 μM), was added to

137   the extracellular solution to block inhibitory synaptic transmission. The membrane resistance

138   was ~30 MΩ, and the synaptic currents with amplitude of 10−150 pA were analysed using a

139   custom code written in MATLAB (Mathworks).

140

141   **2.6 Fluorescent calcium imaging**

142   Cultured neurons were loaded with a fluorescence calcium indicator Cal-520 AM (AAT

143   Bioquest).[12] The cells were first rinsed in HEPES-buffered saline (HBS) containing 128 mM

144   NaCl, 4 mM KCl, 1 mM $CaCl_2$, 1 mM $MgCl_2$, 10 mM D-glucose, 10 mM HEPES, and 45 mM

145   sucrose, and subsequently incubating in HBS containing 2 μM Cal-520 AM for 30 min at 37 °C.

146   The cells were then rinsed in fresh HBS and were imaged on an inverted microscope (IX83,

147   Olympus) equipped with a 20× objective lens (numerical aperture, 0.70), a light-emitting diode

148   light source (Lambda HPX, Sutter Instrument), a scientific complementary metal-oxide

149   semiconductor camera (Zyla 4.2, Andor), and an incubation chamber (Tokai Hit). All recordings

150   were performed at 14−18 DIV, while incubating in HBS at 37 °C. In some experiments,

151   GsMTx-4 (Peptide Institute 4393-s) was added to the HBS to inhibit SACs.[29] Each recording

152   was performed for 10 min at a frame rate of 10 Hz.

153

154   **2.7 Statistical analysis**

155   The results are presented as mean ± S.D. unless otherwise as stated in the main text. Samples

156   sizes (n) are also presented at each section in the text. Statistical significance of the mean values

157   between two groups were compared using Student's t-tests.

158

159

160   **3. Results and discussion**

161   **3.1 Material properties of silicone scaffolds**

162   The elastic scaffolds for neuronal culture were prepared with two types of PDMS, i.e. Sylgard

163   184 mixed at a ratio of 50:1 (hereafter referred to as 'soft') and Sylgard 527 mixed at a ratio of

164   5:4 (hereafter referred to as 'ultrasoft'). We first prepared the PDMS in glass petri dishes and

165   determined their elastic moduli by the spherical indentation method[27,28] (Fig. 1). The elastic

166   moduli of soft and ultrasoft PDMS were determined to be 13.6 ± 1.1 kPa ($n = 4$) and 0.5 ± 0.03

167   kPa ($n = 5$), respectively (Fig. 1c). The values are in good agreement with previous studies,[24,27]

168   and the elastic modulus of the ultrasoft PDMS was nearly equal to that of brain tissue.[21]

169   We next evaluated the wettability of the PDMS surface by measuring water contact

170   angles. Neurons require the scaffold surface to be coated with cationic molecules, such as PDL.

171   However, the strong hydrophobicity of as-prepared PDMS prevents the molecules from stably

172   adsorbing on the surface.[30] Therefore, the samples were exposed to air plasma for a designated

173   amount of time, which hydrophilizes the PDMS surface by substituting methyl groups with

174   hydroxyl groups.[31] The changes in water contact angle θ of the soft and ultrasoft PDMS upon

175   the plasma treatment are shown in Fig. 2a. Prior to the plasma treatment, the PDMS surface was

176   hydrophobic, and θ were measured to be 127.6 ± 6.6 and 123.9 ± 5.1 ($n = 40$) for the soft and

177   ultrasoft PDMS, respectively. The hydrophilicities of samples increased with the plasma

178   exposure time. For the cell-culture experiment, samples exposed to the plasma for 10 s were

179   used in order to minimize the effect of surface vitrification and cracking.[31,32] It has also been

180   previously studied by MacNearney et $al.$[32] that the elastic modulus of Sylgard 527 did not

181   change upon a plasma treatment for less than 10 s, although a plasma treatment for more than

182   30 s resulted in a significant increase in the elastic modulus.

183   The hydrophilized surface was finally coated with PDL, and rat cortical neurons were

184   cultured on the substrates. As shown in Fig. 2a, θ for the soft and ultrasoft PDMS immediately

185   after the 10 s plasma treatment were significantly different. However, the values of θ for the two

186   scaffolds were found to converge after the PDL and the subsequent immersion in the neuronal

187   plating medium (Fig. 2b). This suggests that the surfaces were chemically consistent between

188   the two substrates and validates the comparison of the two substrates focusing solely on their

189   mechanical properties. Representative micrographs of the rat cortical neurons cultured on the

190   soft and ultrasoft PDMS are shown in Figs. 2c–e. Plain glass coverslips coated with PDL were

191   used as controls. The cell bodies of the neurons were well spread, and the neurites uniformly

192   covered the entire surface. In order to compensate for the difference in cell affinity between

193   glass and PDMS, initial plating density was increased 1.5-fold for the two PDMS scaffolds to

194   achieve a constant attachment density of ~950 cells/mm² (Fig. 2f).

195

196   **3.2 Reduction of excitatory synaptic currents on ultrasoft scaffolds**

197   Previous work has shown that the amplitude of excitatory postsynaptic current (EPSC) in

198   hippocampal neurons cultured on Sylgard 184 with E = 457 kPa was significantly higher than

199   that of neurons on Sylgard 184 with E = 46 kPa.[27] To investigate whether a further reduction of

200   substrate stiffness to mimic that of the brain tissue (E ~ 0.5 kPa) influences the synaptic

201   strengths, we compared the amplitude and frequency of spontaneous EPSC (sEPSC) in neuronal

202   networks grown on the soft (E = 14 kPa) and ultrasoft (E = 0.5 kPa) PDMS. sEPSC was

203   recorded from cultured cortical neurons at 14−18 DIV under whole-cell patch clamp. To inhibit

204   spontaneous inhibitory transmissions, a $GABA_A$ receptor blocker, bicuculline (10 μM), was

205   added to the extracellular solution during recording

206   Representative traces from neurons cultured on glass, soft PDMS, and ultrasoft PDMS

207   are shown in Figs. 3a–c, respectively. The amplitude of sEPSC observed in the neurons on soft

208   substrates was 15% lower than those on glass substrates [soft: 23.5 ± 4.1 pA (n = 13), glass:

209   27.8 ± 7.0 pA (n = 11)]. sEPSC amplitude in neurons on ultrasoft substrates was further reduced

210   from those on soft substrates and was approximately 30% lower than those on glass substrates

211   [ultrasoft: 20.4 ± 2.3 pA (n = 12)]. In addition, the frequency of sEPSC from the neurons on soft

212   and ultrasoft substrates was significantly lower than that on glass substrates (ultrasoft: 8.7 ± 3.3

213   Hz, soft: 9.7 ± 3.3 Hz, glass: 13.3 ± 5.6 Hz). These data are summarized in Figs. 3d and 3e.

214   These results indicate that ultrasoft substrates that resemble the elastic moduli of brain tissues

215   suppress the excitatory synaptic strength in cultured cortical neurons. The molecular mechanisms

216   underlying the observations are further investigated and discussed in section 3.4.

217

218   **3.3 Suppression of neural synchrony on ultrasoft scaffolds**

219   Next, fluorescence calcium imaging was used to quantify the difference in the spontaneous

220   firing patterns of neuronal networks on respective substrates. Representative traces of relative

221   fluorescence intensity ($\Delta F/F_o$) from single neurons are shown in Figs. 4a–c. On the glass surface,

222   the peak amplitude of the calcium transients was 0.42 ± 0.01, and the rate was 9.7 ± 0.2

223   events/min (mean $\pm$ S.E.M.; $n = 500$). Both the peak amplitude and the event rate were

224   significantly reduced on the soft PDMS (0.37 ± 0.01 and 7.1 ± 0.3 events/min, respectively; $n =$

225   500). On the ultrasoft substrates, both the amplitude and rate were further reduced as compared

226   to the soft substrate and the control (0.27 ± 0.01 and 5.5 ± 0.2 events/min, respectively; $n = 500$).

227   The reduction is likely to be caused by the reduction in the excitatory synaptic strength. These

228   data are summarized in Figs. 4d and 4e.

229   In order to analyse the degree of neural correlations in the spontaneous activity, we

230   evaluated the correlation coefficient, r_{ij}, between neurons i and j, as:

$$r_{ij} = \frac{\Sigma_t(f_i(t) - \overline{f_i})(f_j(t) - \overline{f_j})}{\sqrt{\Sigma_t(f_i(t) - \overline{f_i})^2}\sqrt{\Sigma_t(f_j(t) - \overline{f_j})^2}},$$ (2)

231   where $f_i(t)$ is the relative fluorescence intensity of cell i at time t, and the overline represents

232   time average. Then, we compared their mean, $\overline{r} = (\Sigma_{i,j(i \neq j)} r_{ij})/N^2$, where $N (= 50)$ is the total

233   number of analysed neurons on respective substrates. Although no significant difference in $\overline{r}$

234   was observed between glass and soft substrates, the value was significantly lower in the

235   neuronal network grown on the ultrasoft scaffold (Fig. 4f). These results show that excessive

236   neural synchronization was suppressed by reducing the scaffold stiffness to 0.5 kPa.

237   The results obtained in this work are in agreement with the previous study, which

238   showed that a stiff PDMS substrate with $E = 457$ kPa increased hippocampal neuronal network

239   activity as compared to a PDMS substrate with $E = 46$ kPa.[27] However, no discernible change in

240   network synchrony was observed within the range of the elasticities investigated by the previous

241   study. In the present study, we found that the non-physiological bursting activity is suppressed,

242   and the mean correlation coefficient significantly decreases when the elastic modulus of the

243   scaffold is further reduced to 0.5 kPa. Thus, Sylgard 527 is a promising scaffold for suppressing

244   the hypersynchrony in neuronal culture.

245

246   **3.4 Molecular mechanism of the scaffold effect**

247   The above results show that the ultrasoft scaffold weakens the excitatory synaptic strength and

248   reduces the synchrony in the neuronal network activity. We hypothesized that SACs, whose

249   activity is downregulated on softer substrates,[33] would be the underlying molecular mechanism

250   and investigated the effect of its pharmacological blockade on the neuronal network activity.

251   GsMTx-4 is a selective antagonist for SACs with an equilibrium constant of

252   approximately 500 nM.[29,34] We first investigated the effect of reducing SAC activity in neurons

253   on glass substrates. Bath application of GsMTx-4 at a concentration of 250 nM was found to

254   reduce the peak amplitude and the rate of spontaneous calcium transients [0.30 ± 0.01 and $4.2 \pm$

255   0.1 events/min (mean $\pm$ S.E.M.), respectively; Fig. 5]. When GsMTx-4 was applied at a higher

256   concentration of 500 nM, the rate was further reduced to 0.24 ± 0.01 events/min (Fig. 5b), while

257   the peak amplitude did not significantly vary from the value observed at 250 nM (Fig. 5a).

258   These results indicate that the fraction of active SACs in the neuronal plasma membrane plays a

259   key role in the generation of spontaneous bursting events and the size of individual events.

260   We next examined the impact of GsMTx-4 application on cortical neurons grown on

261   the PDMS substrates. Application of GsMTx-4 at a concentration of 250 nM reduced the rate of

262   spontaneous calcium transients down to 0.62 ± 0.06 and 0.42 ± 0.02 events/min on the soft and

263   ultrasoft substrates, respectively (Fig. 5b). Therefore, the dose of GsMTx-4 required to reduce

264   the spontaneous occurrence of the calcium transients below 1.0 event/min was lower than that

265   for the neurons on the glass substrate. This suggests that the difference in the baseline level of

266   SAC activation is a molecular mechanism that contributes to the alteration in neuronal network

267   activity depending on scaffold stiffness.

268   Penn et al.[35] previously showed that synchronized network activity in cultured

269   hippocampal neurons decreased with extracellular calcium concentration, which was discussed

270   to be caused by a reduction in presynaptic vesicle release probability. Considering that SACs

271   permeate calcium ions,[36] the decrease in SAC activation could underlie the reduction in sEPSC

272   amplitude and frequency, and neuronal synchrony on ultrasoft substrates.[35,37] Another

273   possibility is that the influx of sodium ions through SACs[36] could directly enhance neuronal

274   excitability independent of the modulation of synaptic strength (e.g. through facilitation of

275   action potential generation). Finally, a mechanism independent of SACs could also have a role.

276   A recent study reported that stiff substrates increase the number of synapses and reduce

277   voltage-dependent Mg^{2+} blockade in N-methyl-D-aspartate receptors, which lead to higher

278   postsynaptic activity in cultured hippocampal neurons.[38] Figure 6 summarizes the above

279   discussion concerning the underlying molecular mechanisms for the suppression of

280   hypersynchrony on the ultrasoft substrate.

281

282   **3.5 Mechanobiology of neuronal cells**

283   Understanding of cellular mechanosensitivity has advanced rapidly since Engler et al.[22] found in

284   2006 that mesenchymal stem cells commit to the lineage specified by scaffold elasticity. With

285   neuronal cells, studies during the last decade have shown that the stiffness of scaffolds affects

286   multiple properties of cultured neurons, including neuritogenesis, neurite outgrowth, branching,

287   and axon pathfinding.[39-41] For instance, Sur et al.[39] has used mouse hippocampal neurons

288   cultured on peptide amphiphile gels to show that the growth rate of neurites in immature

289   neurons significantly increased on scaffolds with lower elastic modulus. The neurite outgrowth

290   of rat spinal cord neurons was also found to be accelerated on softer substrates.[40]

291   Although the molecular mechanism behind the mechanosensitive responses yet remain

292   to be fully elucidated, more recent works have identified that SACs, including the Piezo1

293   channels, are primarily responsible for the effects.[41] This was shown, for example, in the

294   pathfinding and branching of axons in Xenopus retinal ganglion cells[41], as wells as in the

295   determination of cell fate in human neural stem cells.[33] In the current work, we showed that the

296   SAC activity also affects the spontaneous network activity of cultured cortical neurons,

297   providing novel insights into the mechanobiology of neuronal cells and the role of SACs

298   therein.

299

300   **4. Conclusions**

301   We established a protocol for culturing primary cortical neurons on an ultrasoft PDMS gel that

302   mimics the elasticity of brain tissues and investigated the impact of the biomimetic scaffold on

303   synaptic strength and spontaneous activity patterns. Our study showed that the ultrasoft

304   substrate reduces the amplitude of sEPSCs (Fig. 3) that are excessively strong in the *in vitro*

305   cultures. This led to significant reduction in the peak fluorescence amplitude and event rate of

306   spontaneous network bursts on the ultrasoft substrate as compared to the glass substrate (Fig. 4).

307   No significant difference in the correlation of neuronal network activity was observed on the

308   scaffolds with $E > 13.5$ kPa. In contrast, this value was significantly lower for the neuronal

309   network grown on the scaffold with $E = 0.5$ kPa (Fig. 4f), a stiffness similar to that of brain

310   tissue. This is the first evidence that the ultrasoft scaffold with biomimetic elasticity effectively

311   suppresses the hypersynchrony in the spontaneous network activity. A difference in the baseline

312   activation of SACs underlie these stiffness-dependent changes in synaptic transmission and

313   neuronal network activity.

314   The ultrasoft PDMS scaffold offers a mechanically biomimetic culture platform that is

315   beneficial in suppressing the synchronous bursting in neuronal cultures. Moreover, it is a useful

316   platform to study the influence of mechanical cues on neuronal network development. Further

317   work is necessary to fully suppress the synchronized bursting in neuronal cultures. This could

318   be accomplished by integrating cell micropatterning technology with ultrasoft scaffolds or by

319   adding external noise to fill in for functional interactions between brain regions.[12,13]

320

321   **Conflicts of interest**

322   There are no conflicts to declare.

323

324   **Acknowledgements**

References

[1] K. H. Benam, S. Dauth, B. Hassell, A. Herland, A. Jain, K.-J. Jang, K. Karalis, H. J. Kim, L. MacQueen, R. Mahmoodian, S. Musah, Y. Torisawa, A. D. van der Meer, R. Villenave, M. Yadid, K. K. Parker and D. E. Ingber, *Annu. Rev. Pathol. Mech. Dis.*, 2015, **10**, 195-262.

[2] G. Quadranto, J. Brown and P. Arlotta, *Nat. Med.*, 2016, **22**, 1220-1228.

[3] A. Skardal, S. V. Murphy, M. Devarasetty, I. Mead, H-W. Kang, Y-J. Seol, Y. S. Zhang, S.-R. Shin, L. Zhao, J. Aleman, A. R. Hall, T. D. Shupe, A. Kleensang, M. R. Dokmeci, S. J. Lee, J. D. Jackson, J. J. Yoo, T. Hartung, A. Khademhosseini, S. Soker, C. E. Bishop and A. Atala, *Sci. Rep.*, 2017, **7**, 8837.

[4] D. A. Wagenaar, J. Pine and S. M. Potter, *BMC Neurosci.*, 2006, **7**:11, 1271-2202.

[5] J. Soriano, M. Rodríguez Martínez, T. Tlusty and E. Moses, *Proc. Natl. Acad. Sci. U.S.A.*, 2008, **105**, 13758-13763.

[6] J. G. Orlandi, J. Soriano, E. Alvarez-Lacalle, S. Teller and J. Casademunt, *Nat. Phys.*, 2013 **9**, 582-590.

[7] H. Yamamoto, S. Kubota, Y. Chida, M. Morita, S. Moriya, H. Akima, S. Sato, A. Hirano-Iwata, T. Tanii and M. Niwano, *Phys. Rev. E*, 2016, **94**, 012407.

[8] P. Golshani, J. T. Goncalves, S. Khosahkhoo, R. Monstany, S. Smirnakis and C. Portera-Cailliau, *J. Neurosci.*, 2009, **29**, 10890-10899.

[9] J. K. Miller, I. Ayzenshtat, L. Carrillo-Reid and R. Yuste, *Proc. Natl. Acad. Sci. U.S.A.*, **8**, E4053-E4061 (2014).

[10] E. M. Izhikevich, *Neural Comput.*, 2006, **18**, 245-282.

[11] H. Ju, M. R. Dranias, G. Banumurthy and A. M. J. VanDongen, *J. Neurosci.*, 2015, **35**, 4040-4051.

354 [12] H. Yamamoto, S. Moriya, K. Ide, T. Hayakawa, H. Akima, S. Sato, S. Kubota, T. Tanii, M.

355   Niwano, S. Teller, J. Soriano and A. Hirano-Iwata, *Sci. Adv.*, 2018, **4**, eaau4914.

356 [13] K. P. Dockendorf, I. Park, P. He, J. C. Princípe and T. B. DeMarse, *BioSystems*, 2009, **95**,

357   90-97.

358 [14] E. M. Izhikevich, J. A. Gally and G. M. Edelman, *Cereb. Cortex*, 2004, **14**, 933-944.

359 [15] J. Zierenberg, J. Wilting and V. Priesemann, *Phys. Rev. X*, 2018, **8**, 031018.

360 [16] A. K. Vogt, L. Lauer, W. Knoll and A. Offenhäusser, *Biotechnol. Prog.*, 2003, **19**,

361   1562-1568.

362 [17] S. Song, P. J. Sjöström, M. Reigl, S. Nelson and D. B. Chklovskii, *PLoS Biol.*, 2005, **3**,

363   e68.

364 [18] H. Yamamoto, R. Matsumura, H. Takaoki, S. Katsurabayashi, A. Hirano-Iwata and M.

365   Niwano, *Appl. Phys. Lett.*, 2016, **109**, 043703.

366 [19] G. V. Lubarsky, M. R. Davidson and R. H. Bradley, *Surf. Sci.*, 2004, **558**, 135-144.

367 [20] N. Soga, *J. Non-Cryst. Solids*, 1985, **73**, 305-313.

368 [21] N. D. Leipzig and M. S. Shoichet, *Biomaterials*, 2009, **30**, 6867-6878.

369 [22] A. J. Engler, S. Sen, H. L. Sweeney and D. E. Discher, *Cell*, 2006, 126, 677-689.

370 [23] T. Zhang, T. Gong, J. Xie, S. Lin, Y. Liu, T. Zhou and Y. Lin, *ACS Appl. Mater.*

371   *Interfaces*, 2016, **8**, 22884-22891.

372 [24] C. Moraes, J. M. Labuz, Y. Shao, J. Fu and S. Takayama, *Lab Chip*, 2015, **15**, 3760-3765.

373 [25] M. P. Wolf, G. B. Salieb-Beugelaar and P. Hunziker, *Prog. Polym. Sci.*, 2018, **83**, 97-134.

374 [26] H. Yamamoto, L. Grob, T. Sumi, K. Oiwa, A. Hirano-Iwata and B. Wolfrum, *Adv. Biosys.*,

375   2019, **3**, 1900130.

376 [27] Q.-Y. Zhang, Y.-Y. Zhang, J. Xie, C.-X. Li, W.-Y. Chen, B.-L. Liu, X.-a. Wu, X.-N. Li, B.

377   Huo, L.-H. Jiang and H.-C. Zhao, *Sci. Rep.*, 2014, **4**, 6215.

378   [28] M. G. Zhang, Y.-P. Cao, G.-Y. Li and X.-Q. Feng, *Biomech. Model. Mechanobiol.*, 2014,

379   **13**, 1-11.

380   [29] T. M. Suchyna, J. H. Johnson, K. Hamer, J. F. Leykam, D. A. Gage, H. F. Clemo, C. M.

381   Baumgarten and F. Sachs, *J. Gen. Physlol.*, 2000, **115**, 583-598.

382   [30] K. Kang, I. S. Choi and Y. Nam, *Biomaterials*, 2011, **32**, 6374-6380.

383   [31] N. Y. Adly, H. Hassani, A.Q. Tran, M. Balski, A. Yakuschenko, A. Offenhäusser, D.

384   Mayer and B. Wolfrum, *Soft Matter*, 2017 **13**, 6297-6303.

385   [32] D. MacNearney, B. Mak, G. Ongo, T. E. Kennedy and D. Juncker, *Langmuir*, 2016, **32**,

386   13525-13533.

387   [33] M. M. Pathak, J. L. Nourse, T. Tran, J. Hwe, J. Arulmoli, D. T. T. Le, E. Bernardis, L. A.

388   Flanagan and F. Tombola, *Proc. Natl. Acad. Sci. U.S.A.*, 2014, **111**, 16148-16153.

389   [34] C. L. Bowman, P. A. Gottlieb, T. M. Suchyna, Y. K. Murphy and F. Sachs, *Toxicon*, 2007,

390   **49**, 249-270.

391   [35] Y. Penn, M. Segal and E. Moses, *Proc. Natl. Acad. Sci. U.S.A.*, 2016, **113**, 3341-3346.

392   [36] F. B. Kalapesi, J. C. H. Tan and M. T. Coroneo, *Clin. Exp. Optom.*, 2005, **33**, 210-217.

393   [37] N. R. Hardingham, N. J. Bannister, J. C. A. Read, K. D. Fox, G. E. Hardingham and J. J. B.

394   Jack, *J. Neurosci.*, 2006, **26**, 6337-6345.

395   [38] Y. Yu, S. Liu, X. Wu, Z. Yu, Y. Xu, W. Zhao, I. Zavodnik, J. Zheng, C. Li and H. Zhao,

396   *ACS Biomater. Sci. Eng*, 2019, **5**, 3475-3482.

397   [39] S. Sur, C. J. Newcomb, M. J. Webber and S. I. Stupp, *Biomaterials*, 2013, **34**, 4749-4757.

398   [40] F. X. Jiang, B. Yurke, R. S. Schloss, B. L. Firestein and N. A. Langrana, *Tissue Eng. Part

399   A*, 2010, **16**, 1873-1889.

19

400   [41] D. E. Koser, A. J. Thompson, S. K. Foster, A. Dwivedy, E. K. Pillai, G. K. Sheridan, H.

401   Svoboda, M. Viana, L. F. Costa, J. Guck, C. E. Holt and K. Franze, *Nat. Neurosci.*, 2016,

402   **19**, 1592-1598.

403   **Figure captions**

404   **Fig. 1.** Mechanical properties of PDMS. (a) Schematic illustration of the spherical indentation

405   apparatus. (b) Load-displacement curves for soft (*left*) and ultrasoft (*right*) PDMS. Open circles

406   represent the measured data, and the solid curve the fit with Eq. (1) ($r = 0.9999$ for both

407   samples). For the data points, every 50th point is plotted for clarity. (d) Measured elastic moduli

408   of soft and ultrasoft PDMS. Error bars, S.D. *** $p < 0.001$ (two-tailed *t*-test).

409

410   **Fig. 2** Culturing primary neurons on PDMS. (a) Change in water contact angles of soft and

411   ultrasoft PDMS upon exposure to air plasma. (b) Water contact angles measured after plasma

412   irradiation for 10 s, after coating with PDL, and after immersion in the plating medium

413   overnight. The surfaces of both samples were superhydrophilic after the immersion in the

414   plating medium, and thus the data are plotted as 0°. No significant difference was found

415   between the soft and ultrasoft substrates for the datapoints not marked with asterisks. (c–e)

416   Primary cortical neurons cultured on (c) glass, (d) soft, and (e) ultrasoft scaffolds. Scale bars, 50

417   μm. (f) Average cell densities on the glass, soft, and ultrasoft substrates. Error bars, S.D. * $p <$

418   0.05; ** $p < 0.01$; *** $p < 0.001$ (two-tailed *t*-test).

419

420   **Fig. 3.** Effects of elastic modulus on sEPSC. (a–c) Representative recordings of spontaneous

421   EPSCs on (a) glass, (b) soft, and (c) ultrasoft scaffolds. (d and e) The mean values of the

422   amplitude (d) and frequency (e) of sEPSCs on respective surfaces. Error bars, S.D. * $p < 0.05$;

423   ** $p < 0.01$ (one-tailed *t*-test).

424

425   **Fig. 4**. Impact of substrate stiffness on network activity of cultured cortical neurons. (a–c)

426   Fluorescence intensity traces of representative neurons on (a) glass, (b) soft, and (c) ultrasoft

427   scaffolds. Fluorescence micrographs are shown on the right. Scale bars, 100 μm. (d and e)

428   Average peak amplitudes (d) and frequency of bursting events (e) on respective substrates. (f)

429   Mean correlation coefficient (mean CC) of neural activity on respective substrates. Error bars,

430   S.E.M. * $p < 0.05$; ** $p < 0.01$; *** $p < 0.001$ (two-tailed t-test).

431

432   **Fig. 5**. Impact of the pharmacological blockade of SAC on neuronal network activity. (a and b)

433   Average peak amplitudes (a) and rate of bursting events (b) at various concentrations of

434   GsMTx-4 on respective substrates. Error bars, S.E.M. * $p < 0.05$; ** $p < 0.01$; *** $p < 0.001$

435   (two-tailed t-test).

436

437   **Fig. 6**. Diagram summarizing the present findings and the mechanisms underlying the

438   suppression of hypersynchronous neuronal network activity on soft scaffolds. Abbreviations:

439   SAC, stretch-activated cation channel; NMDAR, N-methyl-D-aspartate receptor; sEPSC,

440   spontaneous excitatory postsynaptic current.
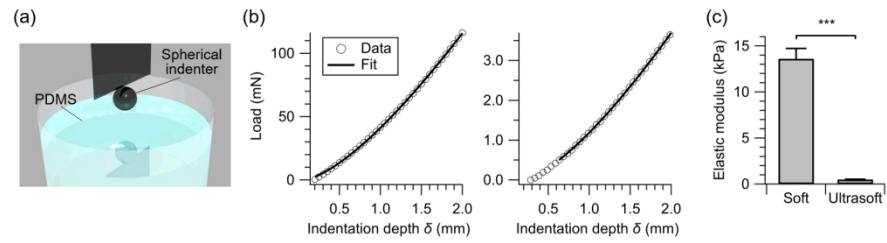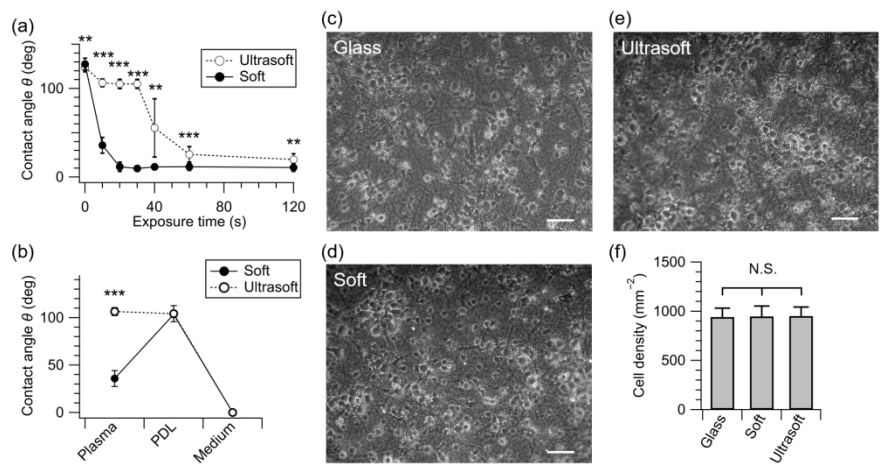
Figure 1

339x190mm (150 x 150 DPI)
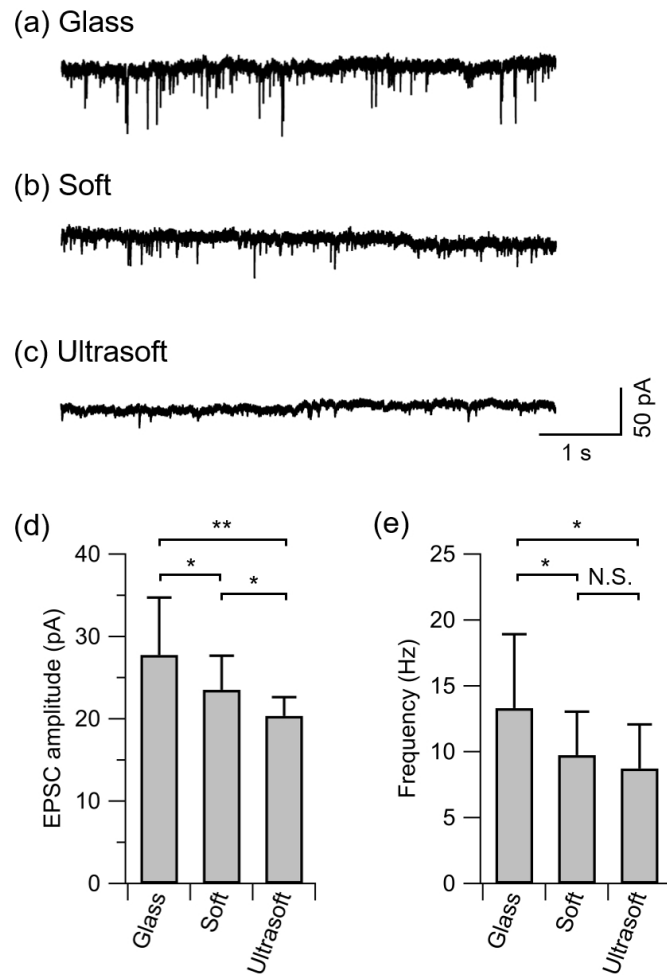
Figure 2

339x190mm (150 x 150 DPI)

(a) Glass

(b) Soft

(c) Ultrasoft

50 pA

1 s

(d)

(e)

Figure 3

181x255mm (150 x 150 DPI)

(a) Glass

(b) Soft

(c) Ultrasoft
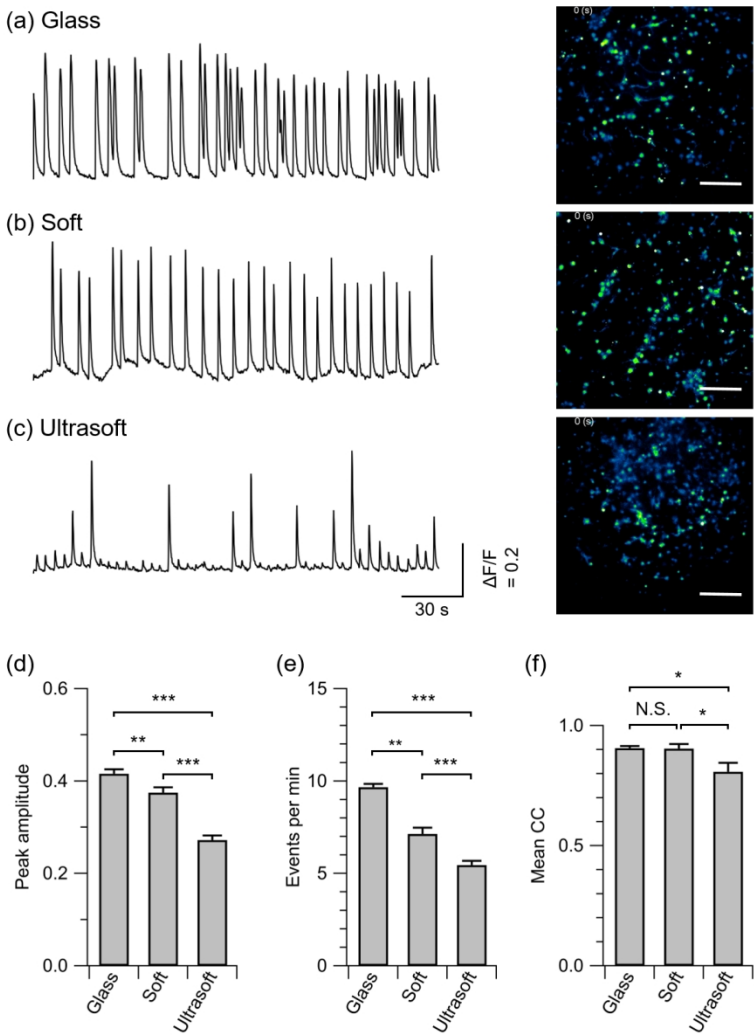
ΔF/F = 0.2

30 s

(d)

(e)

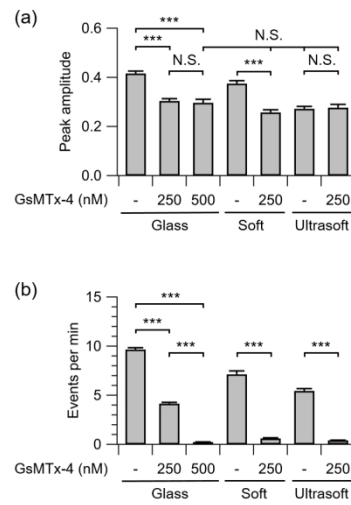(f)

Figure 4

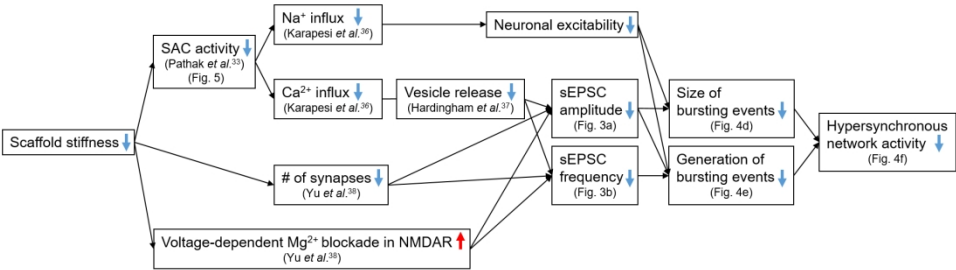234x324mm (150 x 150 DPI)

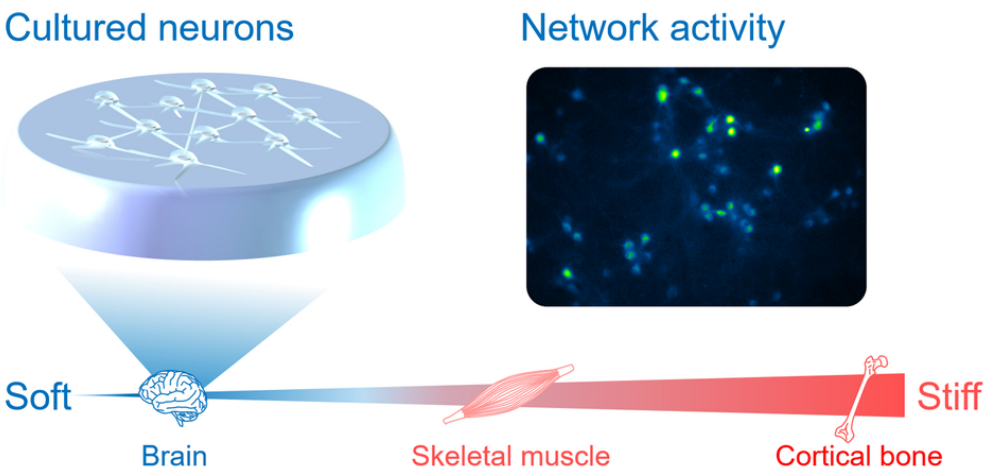Figure 5

339x190mm (150 x 150 DPI)

Figure 6

339x190mm (150 x 150 DPI)

An ultrasoft silicone elastomer as an alternative substrate for neuronal culture is investigated.

79x39mm (300 x 300 DPI)